Geometry Based Other-Sector Interference Modelling for Downlink System Simulations

Lars T. Berger
Department of Communication Technology, Aalborg University,
Fredrik Bajers Vej 7A
9220 Aalborg, Denmark
e-mail: ltb@kom.auc.dk

Troels E. Kolding, Preben E. Mogensen
Nokia Networks, Aalborg R&D
Niels Jernes Vej 10
9220 Aalborg, Denmark
e-mail: troels.kolding@nokia.com
e-mail: preben.mogensen@nokia.com

Laurent Schumacher
Computer Science Institute
University of Namur
Rue Grandgagnage 21
B-5000 Namur, Belgium
e-mail: lsc@info.fundp.ac.be

***Abstract*— An other-sector interference model is developed for the downlink of 3G cellular systems. It is solely based on the cell geometry factor and a user's line of sight angle of connection to a serving base station antenna array. The dependency on just two parameters makes it especially suitable to support a decoupled approach of link and system level simulations, where the link simulations already account for other-sector interference effects. A comparison of the model with a standard 57 sector macrocellular set-up shows that for a 3-sector site deployment, modelling 5 out of 57 sectors with multipath fading characteristics delivers a good trade-off between simulation complexity and other-sector interference modelling accuracy.**

***Keywords*— Other-cell interference, other-sector interference, *G*-factor, quasi-static downlink system simulations.**

I. Introduction

In the quest for higher spectral efficiency and user data rates in wireless communications, the spatial domain and particularly *multiple input multiple output* (MIMO) antenna techniques are receiving a lot of attention in 3GPP and 3GPP2 standardisation fora. In this context accurate link and system modelling methods are essential to assess the applicability of new schemes. While link-level modelling options for MIMO propagation channels are reviewed in [1], this paper focuses on system modelling aspects. To provide guidelines for MIMO system modelling, the *Spatial Channel Model Ad Hoc Group* (SCM-AHG) has recently finished the development of a quasi-static, drop based, spatial channel model [2]. Generally, in *quasi-static* simulations a new user is assigned parameters like

$$\text{User parameters: } \{pathloss,\ shadowing,\ \ldots\ speed\}\ ,$$

that are assumed constant during the entire session. The range and distribution of the user parameters can for instance be obtained by measurements, theoretical derivations, or a combination of these. In terms of obtaining parameters that related to cell geometry, like for example distance dependent path loss or angle of connection related transmit correlation information, a standard approach is to place users in a cellular set-up following a uniform distribution and simply calculate the required information based on their position. After all required user parameters have been assigned they can be used to calculate time evolving channel coefficients, which themselves are used to determine a user's *signal to interference plus noise ratio* (SINR) and finally a user's data throughput. The required operations to determine a user's performance, like minimum mean square error reception and turbo coding, can, however, be very computationally demanding, especially if transmitter and receiver imperfections like nonlinearities, noise factor, and channel estimation errors are considered. To cut down the development time of for example advanced transmit antenna schemes or scheduling algorithms it is therefore beneficial if these time consuming SINR calculations are pre-computed and their results stored in a reusable user performance database. However, the size and eventually the build-up time of such a user database is determined by (i) the number of user parameters and (ii) the sampling resolution of each user parameter (e.g. the number of values defined for each user parameter). Thus, to implement a decoupled look-up approach, which clearly differs from the more uniform approach taken in the SCM-model, it is important to keep the number of dimensions, but also the number of possible values per dimension low. This finite granularity limits the model accuracy, but especially in initial algorithm assessment it is often sufficient for scheme comparison.

The remainder of the paper pursues the decoupled system simulation approach with the specific goal to describe other-sector interference with as few user parameters as possible while maintaining a high degree of simulation accuracy. For this purpose a *scenario simulator* has been developed that exemplifies the process of environment characterisation and parameter extraction using a standard macrocellular environment [3]. For simplicity, the following developments use frequency flat Rayleigh fading, which in terms of multipath dependent interference power variation can be seen as worst case as it does not spread interference energy over several delay taps, i.e. there is no inherent stability due to frequency diversity. The introduced interference modelling approach is, however, not limited to this special flat fading case and was in conjunction with an extension of a frequency selective *spatial channel model* (SCM) link level reference case [2] used in [4] to evaluate the effects of other-sector interference variation on 3G evolution features like link adaptation or channel quality dependent scheduling.

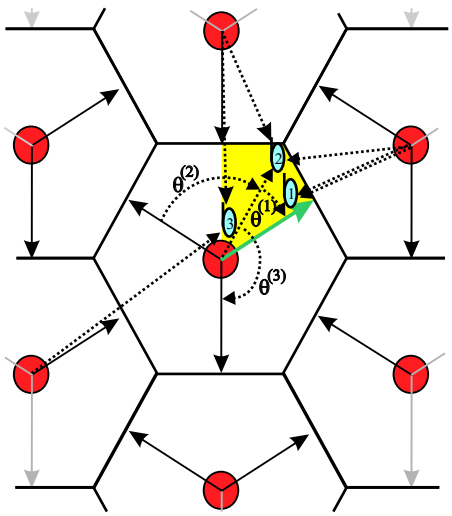

Fig. 1. Excerpt from cellular set-up.

II. System Set-Up and Definitions

The hexagonal cell layout from [2], [3], where the centre base station site is surrounded by two tiers of interfering sites, is adopted

Cite as: L. T. Berger, T. E. Kolding, L. Schumacher, P. E. Mogensen, "Geometry Based Other-Sector Interference Modelling for Downlink System Simulations," *International Symposium on Wireless Personal Multimedia Communications (WPMC)*, Padova, Italy, 2004.

Parameter	Setting
Total number of sectors, N_{sec}	57
Sectors per site, $N_{secpsite}$	3
Site-to-site distance	2800 m
Antenna pattern mean gain, $\overline{L}_{ant}^{(i)}$	14 dBi
Path loss, $L_{path}^{(i)}\left(d^{(i)}\right)$, $d^{(i)}$ in m	$15.3 + 37.6 log_{10}(d^{(i)})$ dB
Shadow fading standard deviation	8 dB
Shadow fading correlation of sectors at the same site	1
Shadow fading correlation of sites	0.5
Full load transmit power, $\overline{P}_{tx}^{(i)}$	43 dBm
Thermal noise density	-174 dBm/Hz
System bandwidth	5 MHz
Terminal noise figure	9 dB

Tab. 1. Cellular set-up parameters.

as an example set-up throughout the following. Each site counts three sectors leading to a total of 57 sectors. The main lobes of the directional sector antenna elements are oriented as indicated by the solid arrows in Fig. 1. The i-th sector's normalised antenna pattern gain $L_{ant}^{(i)}$ towards a mobile user is, as a function of the user's *line of sight angle of connection* (AoC), $\theta^{(i)}$, given as [2], [3]

$$L_{ant}^{(i)}\left(\theta^{(i)}\right) = 10^{\left(-\frac{1}{10}\cdot\min\left\{12\cdot\left(\frac{\theta^{(i)}}{70^{\circ}}\right)^2,20\right\}\right)} \quad . \tag{1}$$

All main cellular set-up parameters are summarised in Table 1. The sectors are grouped in own-site and other-site sectors. Within each group they are indexed in descending order according to their small area mean received power contribution defined as

$$\overline{P}^{(i)} = \overline{L}_{ant}^{(i)} \cdot L_{ant}^{(i)}\left(\theta^{(i)}\right) \cdot L_{path}^{(i)}\left(d^{(i)}\right) \cdot L_{sh}^{(i)} \cdot \overline{P}_{tx}^{(i)} \quad , \tag{2}$$

where $\overline{L}_{ant}^{(i)}$, $L_{path}^{(i)}$, $L_{sh}^{(i)}$ and $\overline{P}_{tx}^{(i)}$ represent the i-th sector's mean antenna gain, path gain, shadow fading gain and full load transmit power respectively. $\overline{L}_{ant}^{(i)}$ and $\overline{P}_{tx}^{(i)}$ are identical for all sectors and $L_{sh}^{(i)}$, modelled log-normally distributed, is identical for all sectors at one site and correlated between all 19 sites using a Cholesky decomposition approach [5]. A user, irrespective of its location, is only connected to the sector from which it receives the strongest small area mean power, i.e. $\overline{P}^{(1)}$.

The instantaneous interference power contribution sum of the *FULL* cellular set-up is

$$P_{FULL} = \sum_{i=2}^{N_{sec}} h^{(i)}\left(h^{(i)}\right)^* \cdot \overline{P}^{(i)} \quad , \tag{3}$$

where $h^{(i)}$ and $\left(h^{(i)}\right)^*$ represent a flat Rayleigh fading channel coefficient and its complex conjugate respectively. Cell statistics are obtained by evaluating the received signal powers from all sectors for a uniform user distribution in the centre cell area, where 'cell' refers to the geometrical shape of a hexagon, but does not relate to a specific coverage area of a single specific sector.

As one quality measure of the other-sector interference model the *interference error ratio* (*IER*) is defined as

$$IER = \frac{P_{FULL}}{P_{model}} \quad , \tag{4}$$

with the ideal case $IER = 1$, i.e. no interference modelling error.

It is further essential that the model covers the same SINR dynamic range as the full set-up. For this purpose a simple *single input single output* (SISO) and a more complex *closed loop transmit diversity mode 1* (CLM1) [6] scheme are implemented and tested in terms of their SINR statistics. Assuming perfect channel estimation and in case of CLM1 error free and instantaneous weight feedback the SINR for both schemes is given by

$$SINR = \frac{N_{sf} \cdot \eta \cdot \widetilde{h}^{(i)}\left(\widetilde{h}^{(i)}\right)^* \cdot \overline{P}^{(1)}}{P_{model}} \quad , \tag{5}$$

where N_{sf} is a user's spreading factor, η is the fraction of full load sector transmit power allocated to a user's data channel, and $\widetilde{h}^{(i)}$ indicates the fading channel coefficient of the weighted channel after transmit antenna combining. The following will use $N_{sf} = 16$ and $\eta = 0.7$. Moreover, it is important to see if the other-sector interference model can capture the effect of *SINR variation* (ΔSINR), where ΔSINR is defined as in [4].

III. Other-sector interference modelling

Looking at existing other-sector interference models it is found that approximating other-sector interference as *additive white Gaussian noise* (AWGN) is, due to its simplicity, a frequently used strategy. To describe the statistics of the other-sector interference contribution the ratio of the serving sector's small area mean received power to all other-sectors' small area mean received powers plus thermal noise is usually defined as the *cell geometry factor* (G-factor) [6]. As the thermal noise floor in the example set-up lies around -98 dBm, and the minimum other-sector interference level lies around -80 dBm, the following defines the G-factor neglecting thermal noise as

$$G = \frac{\overline{P}^{(1)}}{\sum_{i=2}^{N_{sec}} \overline{P}^{(i)}} \quad . \tag{6}$$

Using the assumption that the sum of many equally powered multipath fading interferers can be approximated by their mean the AWGN other-sector interference model writes

$$P_{AWGN} = \frac{1}{G} \cdot \overline{P}^{(1)} \quad . \tag{7}$$

It is interesting to see if this simple model, based on just a single user parameter, i.e. the G-factor, can be extended to encompass more accurate other-sector interference descriptions. For this purpose the model characteristics have been analysed. The average experienced G-factor over the cell area, where 'average' refers to the statistical average over shadow fading realisations, is displayed in Fig. 2. Besides, the G-factor's *cumulative probability density function* (cdf) including shadow fading and seen on 'cell level' is given in Fig. 3(a).

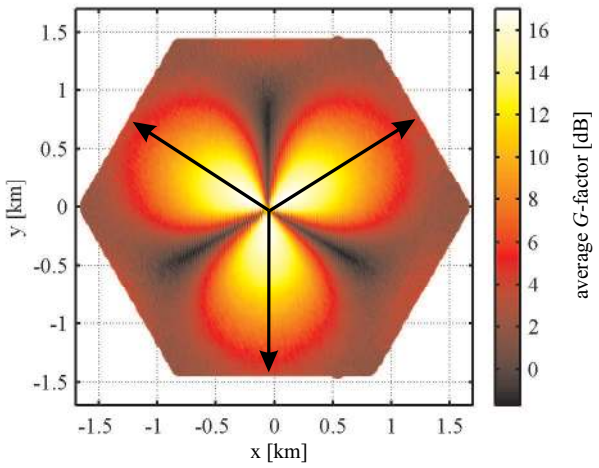

Fig. 2. Average experienced G-factor over cell area.

When modelling multiple transmit antenna systems, like for example CLM1, one might additionally be interested in the

Cite as: L. T. Berger, T. E. Kolding, L. Schumacher, P. E. Mogensen, "Geometry Based Other-Sector Interference Modelling for Downlink System Simulations," *International Symposium on Wireless Personal Multimedia Communications (WPMC)*, Padova, Italy, 2004.

correlation properties of the transmit antennas. Using a similar spatial propagation condition description as in the SCM link level reference cases [2], transmit correlation can be determined as a function of AoC [7]. The probability that a user is served under a specific AoC is given in Fig. 3(b).

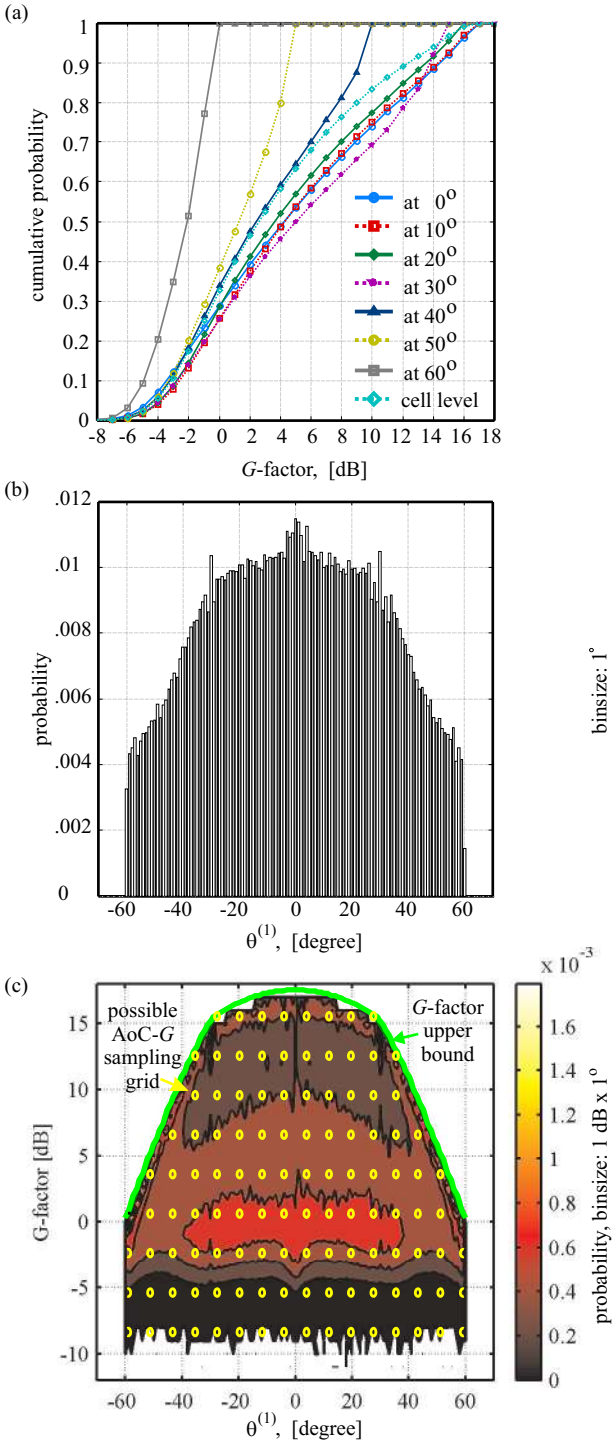

Fig. 3. *G*-factor and AoC distributions.

If transmit correlation information is of importance, the simple AWGN model could be extended by one additional user parameter, e.g. the AoC. However, *G*-factor and AoC-distribution are not independent and their joint probability is plotted in Fig. 3(c), where brighter colours indicate increased probability. A possibly more familiar way of plotting conditional *G*-factor distribution can be seen when revisiting Fig. 3(a), where *G*-factor cdfs are given for a selection of AoCs ranging from 0 to 60°.

It can easily be imagined that the AWGN other-sector interference model is not very accurate, especially at cell locations where in reality only a small number of dominant multipath fading other-sector interferers determine the interference situation. This is reflected in the *IER* evaluation of the AWGN model in Fig. 4, where the absolute of $10log_{10}(IER)$ is plotted at the 95 percentile.

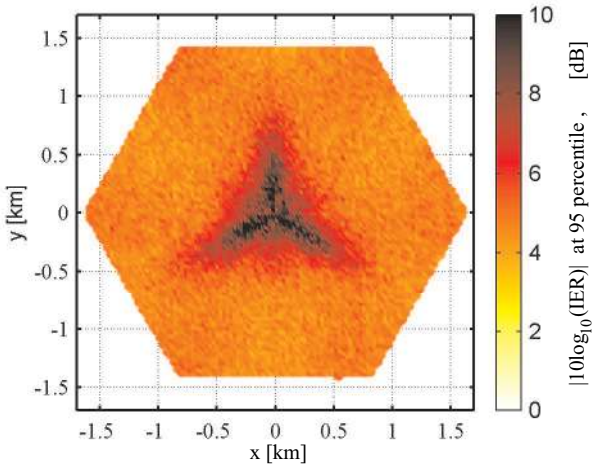

Fig. 4. *IER* performance of the AWGN model over cell area.

The interference power sum P_{AWGN} in the beam overlap regions, i.e. at 90, 210 and 330° close to the cell centre, is off by more than 10 dB in 5% of the cases. Moreover, seen over the whole cell area the AWGN-model was found to cause an interference modelling error that for 5% of the cases exceeds 5.3 dB.

From Fig. 1 the main interferers are identified as the neighbouring own site sectors and the surrounding sectors in the first tier that are reaching the centre cell over their main lobes. Assuming that the *G*-factor and the serving sector's AoC are existing parameters in the user parameter set and using the standard assumption that path gain and shadow fading from all sectors at one site are identical [2], [3], the small area mean received powers of the neighbouring sectors, i.e. $i \in [2,3]$, are simply given as

$$\overline{P}^{(i)} = \frac{L_{ant}^{(i)}\left(\theta^{(i)}\right)}{L_{ant}^{(1)}\left(\theta^{(1)}\right)} \cdot \overline{P}^{(1)} \quad , \tag{8}$$

with the relationship between their AoCs given by

$$\theta^{(2)} = \begin{cases} \theta^{(1)} + 120°, \text{for } \theta^{(1)} \leq 0 \\ \theta^{(1)} - 120°, \text{for } \theta^{(1)} > 0 \end{cases}$$
$$\theta^{(3)} = \begin{cases} \theta^{(1)} - 120°, \text{for } \theta^{(1)} \leq 0 \\ \theta^{(1)} + 120°, \text{for } \theta^{(1)} > 0 \end{cases} \quad . \tag{9}$$

Considering that the own site sectors radiate into the serving sector area mainly over their side lobes they are on average not the strongest interferers. However, their small area mean received power and their transmit correlation are with (8) and (9) directly related to the power and transmit correlation of the serving sector, and their description does not require user parameter set extension.

Using (8) it can be shown that the upper bound of the *G*-factor is purely a function of the selected antenna pattern, i.e.

$$G\left(\theta^{(1)}\right) < \frac{L_{ant}^{(1)}\left(\theta^{(1)}\right)}{\sum_{i=2}^{N_{secpsite}} L_{ant}^{(i)}\left(\theta^{(i)}\right)} \quad . \tag{10}$$

This upper bound is plotted in Fig. 3(c) and can be a valuable delimiter when determining a *G*-factor dimension sampling grid.

As (8) and (9) deliver exact knowledge of the small area mean received powers of the own site sectors the total small area mean

Cite as: L. T. Berger, T. E. Kolding, L. Schumacher, P. E. Mogensen, "Geometry Based Other-Sector Interference Modelling for Downlink System Simulations," *International Symposium on Wireless Personal Multimedia Communications (WPMC)*, Padova, Italy, 2004.

received power sum from all other sites is given by

$$\overline{P}_{other} = \sum_{i=N_{secpsite}+1}^{N_{sec}} \overline{P}^{(i)} = \left(\frac{1}{G} - \sum_{i=2}^{N_{secpsite}} \frac{L^i_{ant}\left(\theta^i\right)}{L^1_{ant}\left(\theta^1\right)}\right) \cdot \overline{P}^{(1)} \quad . \tag{11}$$

The average contribution of the first and second strongest other site interferer, $i \in [4,5]$, to the total other site small area mean received power sum, i.e. $\overline{\mu}^i = E\left\{\frac{\overline{P}^{(i)}}{\overline{P}_{other}}\right\}$, was found to be 0.42 and 0.18 respectively. Their small area mean received powers can therewith be approximated as

$$\overline{P}^{(i)} \approx \widehat{\overline{P}}^{(i)} = \overline{\mu}^{(i)} \cdot \overline{P}_{other} \quad . \tag{12}$$

A similar modelling process could be continued up to N_{sec} sectors, but it will be shown that for the 3-sector site example set-up modelling the two strongest other site sectors delivers an appealing trade-off between model complexity and simulation accuracy.

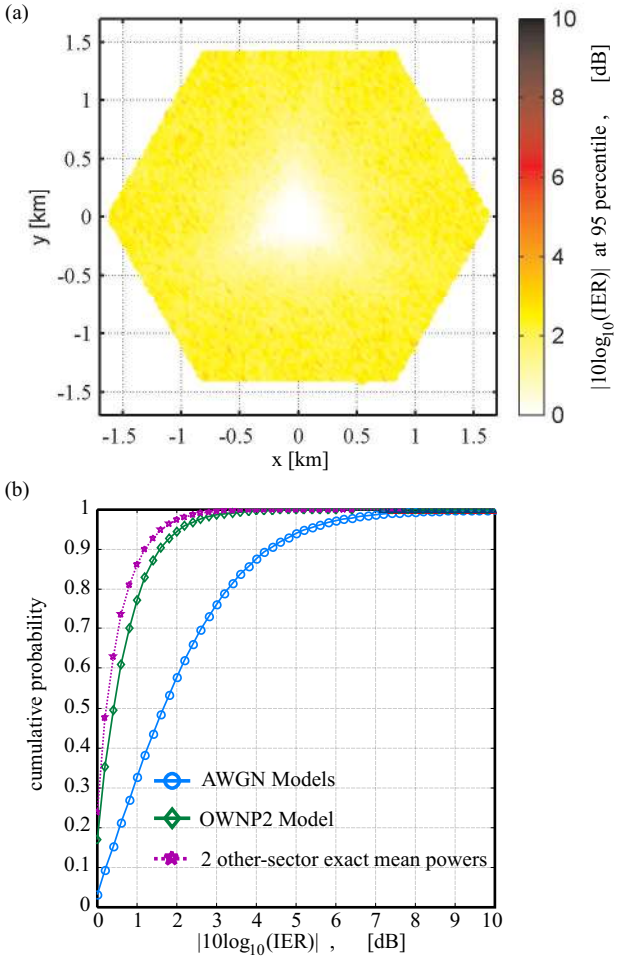

Fig. 5. *IER* performance statistics.

Using (8) and (12) an *own site plus 2 other sector interference model* (OWNP2) based on only the two user parameters, AoC and G, is given by

$$P_{OWNP2} = \left(\sum_{i=2}^{3} \frac{L^{(i)}_{ant}(\theta^{(i)}) h^{(i)} (h^{(i)})^*}{L^{(1)}_{ant}(\theta^{(1)})}\right) \cdot \overline{P}^{(1)} + \left(\sum_{i=4}^{5} h^{(i)} \left(h^{(i)}\right)^* \overline{\mu}^{(i)}\right) \cdot \overline{P}_{other} + \left(1 - \sum_{i=4}^{5} \overline{\mu}^{(i)}\right) \cdot \overline{P}_{other} \quad , \tag{13}$$

and its interference power modelling performance over cell area is displayed in Fig. 5(a).

Comparison with Fig. 4 clearly shows the performance benefit obtained in the cell centre as well as in the cell border regions. The absolute of the 95 percentile *IER* over the whole cell area could be reduced from 5.3 to 2.1 dB. Looking at the *IER* performance cdfs in Fig. 5(b) it can be seen that the power modelling approximation in (12) causes an error of around 0.4 dB with respect to knowing the exact small area mean received powers.

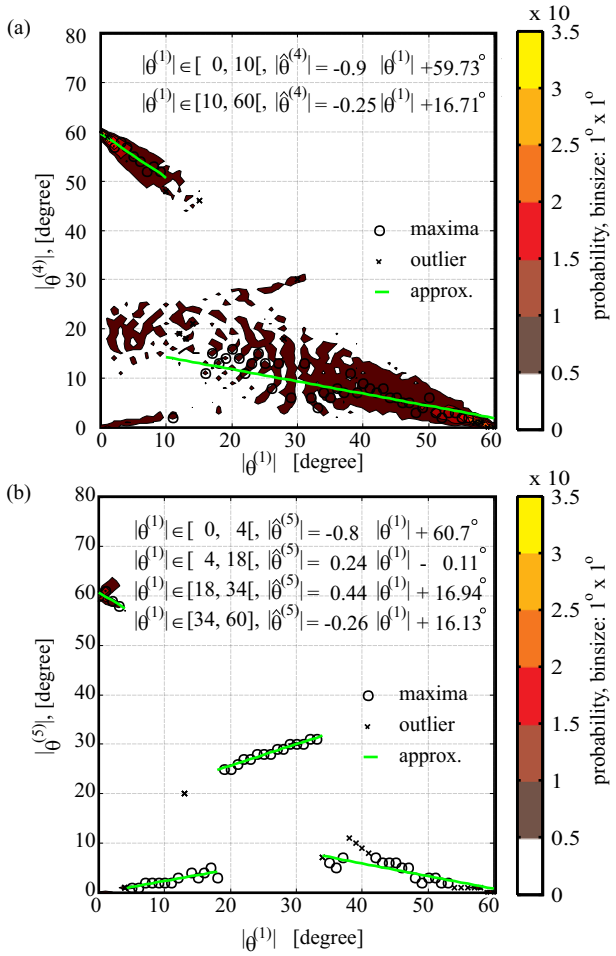

Fig. 6. Joint probability of $|\theta^{(1)}|$ and $|\theta^{(i)}|$, $i \in [4,5]$, and their linear approximation.

For interfering sector transmit correlation modelling a simple relation between absolute out of cell interfering sector AoCs, i.e. $|\theta^{(i)}|$, $i \in [4,5]$, and the absolute of the serving sector's AoC, $|\theta^{(1)}|$, is desirable. Therefore the joint probability densities between $|\theta^{(1)}|$ and $|\theta^{(i)}|$ have been collected. The linear models displayed in Fig. 6 (a) and (b) have been extracted by (i) identification of points with the highest probability ('maxima' & 'outlier'), (ii) selection of linear regression intervals by inspection, (iii) identification of points ('outlier') who's $|\theta^{(i)}|$ deviates by more than the estimated standard deviation from the estimated mean over an interval, and (iiii) linear least square curve fit through the 'maxima' only.

Looking at three example mobile positions in Fig. 1 one can reach an intuitive understanding of these absolute AoC relationships. In position 1, $|\theta^{(1)}|$ is close to 0° while there is a high probability that the other-site interference is received with $|\theta^{(4)}|$ and $|\theta^{(5)}|$ close to 60° as indicated by the dotted arrows pointing at mobile position 1. Along the same lines arguments can be found for position 2 and 3.

To get a feeling which impact these AoC relationships can have on transmit antenna correlation, for example considering a

Cite as: L. T. Berger, T. E. Kolding, L. Schumacher, P. E. Mogensen, "Geometry Based Other-Sector Interference Modelling for Downlink System Simulations," *International Symposium on Wireless Personal Multimedia Communications (WPMC)*, Padova, Italy, 2004.

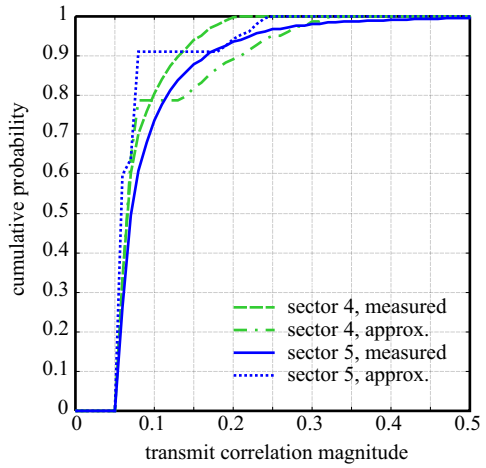

Fig. 7. Transmit correlation statistics, sectors 4 and 5.

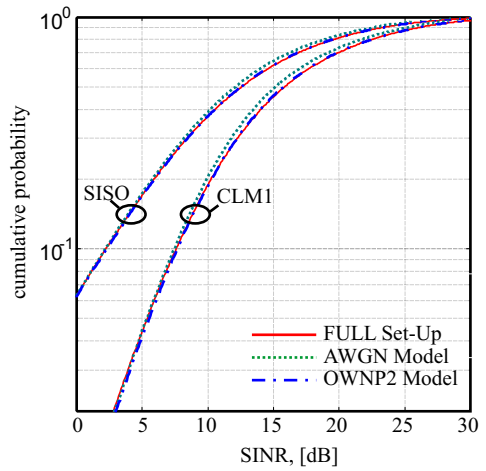

Fig. 8. SINR cdfs for models and full set-up.

Laplacian distributed power azimuth spectrum with an azimuth spread of 5° and a transmit antenna spacing of 10 wavelengths, the transmit correlation cdfs of sector 4 and 5 are given in Fig. 7. It can be seen that the simple linear relations between serving sector AoC and the strongest other site AoCs cannot fully achieve the same transmit correlation distribution. While the model for sector 4 slightly overestimates transmit correlation, the model for sector 5 slightly underestimates it.

To answer the question if the developed other-sector interference model delivers a sufficient trade-off between simulation accuracy and simulation complexity it is important to check how well it meets the desired requirements in terms of modelling the SINR-dynamic range and the SINR variability when for example CLM1 with interfering sector transmit weight updates is deployed. Looking at the SINR cdf in Fig. 8 it is found that AWGN and the OWNP2 model both manage to reach the statistics of the full set-up within a 0.3 dB margin. Whereas 0.3 dB mean SINR difference can in absolute terms lead to approximately 7% cell performance difference it should be considered that the model is intended to compare the relative performance of different algorithms. Based only on the SINR statistics it might be concluded that both models would well be suited. However, it is clear that the temporally stable AWGN model is not able to account for any SINR-variation effects that are caused by interfering sector weight updates. Looking at the ΔSINR statistics of both models and the full set-up in Fig. 9 it can be seen that the OWNP2 model is able to account for interference variation with an accuracy of 0.1 dB. Knowing that such a difference has minimal impact on for example turbo decoder performance and link adaptation [4] it can be concluded that the OWNP2 model is well suited to model other-sector interference.

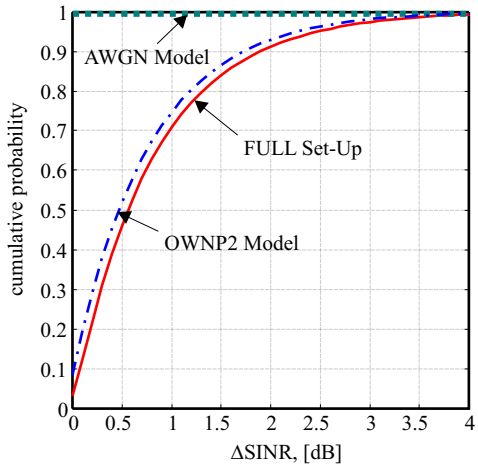

Fig. 9. ΔSINR cdfs for models and full set-up.

With the help of extensive link simulations it was found that an oversampling of the AoC-*G* distribution with 8° AoC and 3 dB *G*-steps, as indicated in Fig. 3(c) does not limit the OWNP2 model performance under the above criteria. Exploiting the symmetry in the AoC-domain, this leads to a database size of 58 traces, one for every AoC-*G* user parameter pair, which can be regarded as a reasonable task considering standard processing power.

IV. Conclusions

An other-sector interference model has been developed solely based on the cell geometry factor and the line of sight angle of connection. Model development was exemplified on a standard regular grid macrocellular set-up with 3-sector sites but is generally extendable to other scenarios as well as higher numbers of modelled interfering sectors. As the model is only based on two varying parameters, it is well suited to support a decoupled link/system simulation approach, where link results including other-sector interference effects are stored in a user performance data base ready for use by a system simulator. Such approach allows for very detailed link simulations including the modelling of real world imperfection while at the same time enabling fast and efficient system level algorithm tests and comparisons.

References

[1] L. Schumacher, L. T. Berger, J. Ramiro-Moreno, and T. B. Sørensen, *Adaptive Antenna Arrays - Trends and Applications*, chapter Propagation Characterization and MIMO Channel Modeling for 3G, pp. pp.377–393, Signals and Communication Technology. Springer, Heidelberg, June 2004.

[2] Spatial Channel Model Ad-Hoc Group, "Spatial Channel Model Text Description", Tech. Rep. SCM-134 v6.0, 3GPP/3GPP2, April 2003.

[3] 3GPP, "Feasibility Study for OFDM for UTRAN enhancement", Technical Specifications TR 25.892 (V0.1.1), Technical Specification Group Radio Access Network, February 2003.

[4] L. T. Berger, T. E. Kolding, P. E. Mogensen, F. Frederiksen, and K. I. Pedersen, "Effects of Other-Sector Interference Variation on Detection, Link Adaptation and Scheduling in HSDPA", in *The Nordic Radio Symposium*, Oulu, Finland, August 2004, accepted for publication.

[5] T. Klingenbrunn and P. Mogensen, "Modelling Cross-Correlated Shadowing in Network Simulations", in *IEEE VTS 50th Vehicular Technology Conference*, September 1999, vol. 3, pp. 1407–1411.

[6] H. Holma and A. Toskala, Eds., *WCDMA for UMTS, Radio Access For Third Generation Mobile Communications*, Wiley, Chichester, UK, second edition, 2002.

[7] L. Schumacher, K. I. Pedersen, and P. E. Mogensen, "From Antenna Spacing to Theoretical Capacities - Guidelines for Simulating MIMO Systems", in *PIMRC*, 2002, pp. 587–592.

Cite as: L. T. Berger, T. E. Kolding, L. Schumacher, P. E. Mogensen, "Geometry Based Other-Sector Interference Modelling for Downlink System Simulations," *International Symposium on Wireless Personal Multimedia Communications (WPMC)*, Padova, Italy, 2004.